Characterization of human epiplakin: RNAi-mediated epiplakin depletion leads to the disruption of keratin and vimentin IF networks

Shyh-Ing Jang*,‡,§, Alexandr Kalinin*, Kaoruko Takahashi, Lyuben N. Marekov and Peter M. Steinert¶

Laboratory of Skin Biology, NIAMS, National Institutes of Health, Bethesda, MD 20892-8023, USA

*These authors contributed equally to this work
‡Present address: Human Craniofacial Genetics Section, CRC, NIDCR, NIH, DHHS, Building 10, Room 5N102, 10 Center Drive, Bethesda, MD 20892-1423, USA
¶This paper is dedicated to the memory of Peter Steinert who initiated and provided great inspiration on this study
§Author for correspondence (e-mail: jangs@mail.nih.gov)

Accepted 16 November 2004
Journal of Cell Science 118, 781-793 Published by The Company of Biologists 2005
doi:10.1242/jcs.01647

Summary

Epiplakin is a member of the plakin family with multiple copies of the plakin repeat domain (PRD). We studied the subcellular distribution and interactions of human epiplakin by immunostaining, overlay assays and RNAi knockdown. Epiplakin decorated the keratin intermediate filaments (IF) network and partially that of vimentin. In the binding assays, the repeat unit (PRD plus linker) showed strong binding and preferentially associated with assembled IF over keratin monomers. Epiplakin knockdown revealed disruption of IF networks in simple epithelial but not in epidermal cells. In rescue experiments, the repeat unit was necessary to prevent the collapse of IF networks in transient knockdown; however, it could only partially restore the keratin but not the vimentin IF network in stably knocked down HeLa cells. We suggest that epiplakin is a cytolinker involved in maintaining the integrity of IF networks in simple epithelial cells. Furthermore, we observed an increase of epiplakin expression in keratinocytes after the calcium switch, suggesting the involvement of epiplakin in the process of keratinocyte differentiation.

Key words: epiplakin, intermediate filaments, keratinocyte

Introduction

Epiplakin was first discovered as an autoantigen in a patient with subepidermal blistering skin disease (Fujiwara et al., 1996). Later it was found in a variety of tissues, such as liver, small intestine, stomach, salivary gland, esophagus and skin (Fujiwara et al., 2001). Based on its deduced protein sequence, it was classified as a member of the plakin family with the presence of plakin-repeat domain (PRD) homologous to the B subdomain of desmoplakin (Green et al., 1990). Plakin family members, including desmoplakin, plectin, envoplakin, periplakin, bullous pemphigoid antigen 1 and microtubule-actin crosslinking factor, have been characterized as cytolinkers involved in the organization of the cytoskeleton (reviewed by Leung et al., 2001; Leung et al., 2002). Plakins are expressed mainly in tissues that are subject to mechanical stress such as epithelia and muscle. In addition, it has been reported that some plakins participate in the development and maintenance of cytoskeletal architecture in neurons (Guo et al., 1995; Lee et al., 2000). Many plakins are present in multiple isoforms and differentially express through alternative splicing in a tissue-specific expression pattern (Brown et al., 1995; Bernier et al., 1996; Elliott et al., 1997). Depending on the type of tissue, each isoform has a distinct interaction with the cytoskeletal networks (Yang et al., 1996; Yang et al., 1999). The importance of these cytolinkers is further highlighted by the impairment of plakins found in patients with autoimmune or inherited diseases. These disorders usually lead to tissue fragility such as that displayed in muscular dystrophy and the skin disease epidemolysis bullosa simplex (Fuchs and Cleveland, 1998).

Most plakins are very large proteins that share certain functional domains such as the actin-binding domain (ABD), plakin domain, coiled-coil rod domain and plakin-repeat domain (PRD). These proteins contribute to the maintenance of tissue integrity by interacting with cytoskeletal filaments and anchoring them to each other and to membrane junction complexes (reviewed by Ruhrberg and Watt, 1997; Fuchs and Karakesisoglou, 2001; Leung et al., 2001; Leung et al., 2002). For instance, desmoplakin interacts with intermediate filaments (IFs) and anchors them to desmosomes (Bornslaeger et al., 2001). Plectin, the most versatile plakin cytolinker with five copies of B subdomains, decorates IF networks in the cytoplasm and co-localizes with cortical actin at focal adhesion contracts (Wiche et al., 1983; Seifert et al., 1992; Wiche et al., 1993). Plectin also plays a major role in linking the IF networks to hemidesmosomes (Borradori and Sonnenberg, 1996; Green and Jones, 1996; Burgeson and Christiano, 1997). It has been shown that the PRD of desmoplakin and plectin plays a critical role in the direct binding of IFs (Stappenbeck and Green, 1992; Steinbock et. al., 2000). In keratinocytes, envoplakin and periplakin, together with involucrin were first characterized as precursors of the cornified cell envelope (CE) (Simon and Green, 1984; Ma and Sun, 1986). Periplakin, when transfected in full length, localizes to desmosomes, interdesmosomal

plasma membrane and IFs (DiColandrea et al., 2000). In addition, the binding of the C terminus of periplakin with IFs has been reported (Kazerounian et al., 2002; van den Heuvel et al., 2002; Karashima and Watt, 2002). Furthermore, full length envoplakin is expressed in aggregates associated with IFs (DiColandrea et al., 2000).

Epiplakin is mostly found in epithelial tissues (Fujiwara et al., 2001; Spazierer et al., 2003). Like other plakin members, epiplakin is a large protein. Both human and mouse epiplakin genes have been reported, and both feature a huge single exon (more than 20 kb) encoding 13-16 PRDs with various sizes of linkers in between (Takeo et al., 2003; Spazierer et al., 2003). The last five to eight repeated units [linker plus B domains; nomenclature according to Fujiwara et al. (Fujiwara et al., 2001)] of epiplakin are virtually identical even at the nucleotide level. However, epiplakin lacks the center coiled-coil rod domain and the amino-terminal globular domain. It was predicted that epiplakin would exist as a single chain molecule in vivo since no dimerization domain was found (Fujiwara et al., 2001). However, the subcellular localization, the biological function and its interaction partners remain unknown.

Knockout studies on some plakins have been well documented. Plectin-null mice showed a phenotype similar to the autosomal recessive skin disease known as epidermolysis bullosa simplex with muscular dystrophy (EBS-MD) (Andrä et al., 1997). The knockout of desmoplakin resulted in embryonic lethality due to the loss of integrity of the extra-embryonic endoderm (Gallicano et al., 2001). After the ablation of bullous pemphigoid antigen 1 (BPAG-1), in mice there was sensory neuron degeneration, and they died at 4-6 weeks (Brown et al., 1995; Guo et al., 1995). While the absence of envoplakin resulted in subtle phenotypes with a slight delay in the formation of the skin barrier (Määttä et al., 2001), the periplakin-null mice developed normally and did not show any skin phenotype (Aho et al., 2004). However, gene ablation of epiplakin through a conventional knockout study has not yet been reported.

In the present study, we have determined the subcellular localization of human epiplakin in cultured epithelial cells by immunofluorescence analysis. We demonstrate the association of epiplakin fragments with keratins and vimentin by overlay binding assays. We also observed, by real-time RT-PCR, the increase of epiplakin expression in keratinocytes as they underwent differentiation. In particular, we used RNAi to effectively reduce the level of epiplakin and conducted rescue experiments with epiplakin fragments in HeLa cells. We provide evidence that epiplakin plays a crucial role in the integrity of IF networks in simple epithelial cells.

Materials and Methods

Generation of cDNA constructs

A 1.8 kb cDNA encompassing the last linker (L12), B repeat (B13) and five additional residues before the stop codon (Table 1) was obtained by RT-PCR using total RNA of HeLa cells as a template. The cDNA was synthesized using 5′-GCACGGAGGAAGCCCAGTCAC (reverse) paired with 5′-ACTTCGACGAGGAGATGAACCGT (forward) by one-step RT-PCR (Invitrogen). The PCR product was cloned into TA vector (Invitrogen) and verified by cycling sequencing. This construct was used as a template to generate fragments with different combinations of B repeat and linker (Table 1). The fragments were subcloned into a pGATEV vector of *Nde*I/*Xho*I sites [a gift from K. Alexandrov (Kalinin et al., 2001)], allowing inducible expression of N-terminal GST fusion proteins. To generate pEGFP-fused epiplakin constructs, the same primers with different linkers (Table 1) were paired with the corresponding reverse primers for PCR to obtain B13, L12 and L12B13 epiplakin fragments. These fragments were first cloned into TA vector and digested with *Sal*I/*Eco*RI, gel cleaned, and cloned into *Xho*I/*Eco*RI sites of pEGFP-C3 (Clontech) to obtain pEGFP-B13, pEGFP-L12 and pEGFP-L12B13. All of the DNA sequences were verified to ensure the coding region was in-frame.

Expression constructs of human keratins 5, 14, 8 and 18 were constructed as follows; the cDNAs were obtained with each corresponding pair of primers (Table 1) by one-step RT-PCR (Invitrogen) using total RNA isolated from HeLa and NHEK (normal human epidermal keratinocytes) cells. All cDNA fragments were first

Table 1. Construction of human epiplakin fragments and full length cDNA of human keratins

cDNA fragment* (accession no.)	Primers used in PCR†	Corresponding amino acid region
Epiplakin: (AB051895)	5′-CTCTACcatatgCAGCTGGCAGGCCGGGG-3′ 5′-GAGGAActcgagTCACTGTAGAGAGAGAGAAAGAAATAGG-3′	4527-5065 (L12-B13)
Epiplakin:	5′-CTCTACcatatgCAGCTGGCAGGCCGGGG-3′ 5′-GCTCATctcgagCTAGCGGCCGGGCTGGTCCTTGGC-3′	4527-4885 (L12)
Epiplakin:	5′-GCCCcatatgCAGGAGAAGATGAGCATCTACCAGG-3′ 5′-GAGGAActcgagTCACTGTAGAGAGAGAGAAAGAAATAGG-3′	4885-5065 (B13)
Keratin 5 (NM_000424)	5′-AGGAACAAGCCcatatgTCTCGCCAGTCAAGT-3′ 5′-GTGACTTGCAGCAGGaagcttGCTCTTGAAGCTCT-3′	1-590 (full length)
Keratin 14 (NM_000526)	5′-ACCTCCCTCCTCTGCcatatgACTACCTGCAGCCGCCAG-3′ 5′-TGAGCGGGGCTGGGCAaagcttGTTCTTGGTGCGAAGGAC-3′	1-472 (full length)
Keratin 8 (NM_002273)	5′-CTCCAGCCTCTcatatgTCCATCAGGGTGACCCAGAAGT-3′ 5′-AGGGGCTGCCGCAgcggccgcCTTGGGCAGGACGTCAG-3′	1-483 (full length)
Keratin 18 (NM_000224)	5′-TCTCTCTCCCCGGACcatatgAGCTTCACCACTCGCTCCACCT-3′ 5′-AGGGTACCCTGCTTCTGCTaagcttATGCCTCAGAACTTTGGTG-3′	1-430 (full length)

*The epiplakin fragments were cloned into pGATEV expression plasmid. Full-length keratin cDNAs were cloned into pET23a plasmid and in frame with His-tag on the C-terminal.

†In each PCR reaction, the upper and lower primers are the sense and antisense oligonucleotides, respectively. The cloning linkers are lowercase. The stop codon of each epiplakin fragment is underlined.

cloned into TA vector, digested with corresponding restriction enzymes and subcloned into pET23a expression vector (Novagen). The human vimentin expression construct was a generous gift from R. Goldman. Human involucrin expression construct was used as previously described (Nemes et al., 1999).

Epiplakin antibody

To generate antibody against human epiplakin, the peptide PGARPQLQDAWRGPREPG, found in several linkers, was synthesized and used as the antigen. Rabbit antiserum was generated by Harlan Bioproducts (Indianapolis, IN). The polyclonal antibody was affinity-purified with UltraLink Immobilization Kit (Pierce). The specificity of epiplakin antibody was characterized by western blotting.

Cell culture and indirect immunofluorescent staining

NHEK (normal human epidermal keratinocytes) cultures, HaCaT cells (gift from E. N. Fusening), HeLa (human cervical carcinoma), COS-7 (African green monkey kidney) and A431 (human epidermoid carcinoma) cells were maintained as previously described (Jang et al., 1996). NHEK-L cells were grown in low calcium (0.05 mM) medium. In NHEK-H cultures, the calcium concentration was raised to 1.2 mM for the initiation of the terminal differentiation of keratinocytes. For immunofluorescent staining, all fixation and staining procedures described below were conducted at room temperature. The cultures grown in the four-chamber slide (Lab-Tek) were fixed with cold methanol (–20°C) for 5 minutes, washed three times with PBS and permeabilized with 0.4% Triton X-100 in PBS solution for 30 minutes. After washing three times with 0.05% Tween 20 in PBS (PBST), cultures were blocked in 5% nonfat milk (Carnation) in PBST for 30 minutes. Cells were incubated with primary antibodies for 1 hour. The following antibodies were used: mouse antibodies against vimentin (1:100), keratin 5 (1:100), keratin 14 (1:100) were from Novocastra; guinea pig polycolonal anti-pan keratin (1:30), mouse anti-actin (1:200) and mouse anti-tubulin (1:200) were from Sigma. After washing, the cells were incubated with secondary antibodies which included goat anti-rabbit, anti-mouse, anti-guinea pig with the FITC-, TRITC-, or Cy5-conjugated IgG (1:300, Jackson Immunoresearch) for 30 minutes. After washing, the cell nuclei were stained with TO-PRO-3 (2 μM; Molecular Probes) in PBST. The control samples included those treated with either secondary antibody alone or with preimmune rabbit serum for epiplakin polyclonal antibody. The slides were mounted with Vector Shield (Vector) and examined using either a Leica DMR fluorescence microscope or an Olympus laser scanning confocal microscope (Fluoview 500) with sequential scanning mode. At least 20 different fields were evaluated and one representative result is shown for each experiment. Images were processed using Adobe Photoshop 7.0.

Expression, purification of keratins, filaments assembly and dot blot overlay assays

The expression and purification of human keratins were the same as described by Fontao et al. (Fontao et al., 2003) except that the proteins were extracted from final pellets by urea buffer (25 mM Tris-HCl, pH 8.0, 500 mM NaCl, 5 mM imidazole, 8 M urea). After an additional centrifugation at 37,500 ***g***, the supernatants were collected and the urea concentration was adjusted to 6 M. Keratins were further purified using a 5 ml Hi-Trap Ni-NTA column (Pharmacia) and eluted by a gradient of 5-500 mM imidazole. Fractions were collected and analyzed by 4-12% Bis-Tris NuPAGE (Invitrogen) and Coomassie Blue staining.

The bacterially expressed K5, K14, K8 and K18 keratins were purified and polymerized into filaments by stepwise dialysis as described previously (Yamada et al., 2003). For overlay binding assays, the recombinant proteins or assembled filaments (1 μg each) were immobilized on a PVDF membrane using Bio-Dot microfiltration apparatus (Bio-Rad). One membrane was stained with 0.1% Amido Black (Sigma). The others were incubated with the indicated recombinant GST-fused epiplakin proteins (5 μg/ml) in blocking solution (5% nonfat milk in PBST) for 1 hour and probed with rabbit anti-GST antibody (Upstate) and goat HRP-conjugated anti-rabbit antibody (Bio-Rad) for 30 minutes. After washing, the membranes were visualized by SuperSignal West Pico Lumino/Enhancer (Pierce) and exposed to X-ray film (MR, Kodak).

Western blot analysis

Cells were collected in lysis buffer as previously described (Jang and Steinert, 2002). After centrifugation at 21,000 ***g*** for 10 minutes at 4°C, the supernatant was collected as a soluble fraction. The pellets were resuspended in NuPAGE LDS sample buffer (1×; Invitrogen), boiled for 10 minutes and centrifuged at 21,000 ***g*** for 5 minutes This supernatant was used as an insoluble fraction that contained mainly the cytokeratins. For immunoblotting, equal amounts of the soluble or insoluble fractions were run on 4-12%, Bis-Tris NuPAGE (Invitrogen) and transferred onto polyvinylidene difluoride (PVDF) membrane. The membranes were blocked and probed either with anti-epiplakin antibody (1:2000) only, or together with mouse anti-β-actin (1:2000, Sigma) or anti-β-tubulin (1:1000, Sigma) antibodies. After washing, the membranes were incubated with HRP-conjugated anti-rabbit antibodies (1:2000) and developed as described above.

Real-time RT-PCR

For reverse transcription (RT), total RNA (1 μg) from HeLa or NHEK cells was first treated with deoxyribonuclease I (Invitrogen) and was reverse transcribed by the gene-specific reverse primer (epiplakin: 5′-TGTTTGTTGCTGGTTTCCTGC; involucrin: 5′-GCGGACCC-GAAATAAGTGG; β-actin: 5′-GCCTTGCACATGCCGG) with SuperScript III reverse transcriptase (Invitrogen) followed by RNase H treatment before proceeding to the PCR reaction. A negative control containing all of the RT reagents except RT enzyme was included. For real-time PCR, the primers and Taqman probes were designed: for epiplakin, forward (5′-AGCTGGTGAGGATGTATAGAACACAC), reverse (5′-TGTTTGTTGCTGGTTTCCTGC) and Taqman probe (5′-ACGGGCACTGCAGACGGTAGCG); for β-actin, forward (5′-ACCATGGATGATGATATCGCC), reverse (5′-GCCTTGCACATG-CCGG), and Taqman probe (5′-CGCTCGTCGTCGACAACGGC); for involucrin, forward (5′-CCAGAGGCCCTCAGATCGT), reverse (5′-GCGGACCCGAAATAAGTGG), and Taqman probe (5′-TCAT-ACAAGGGAAGAGAGAGCCACTGGC). Involucrin was included as a control to monitor the differentiation of keratinocytes, and β-actin served as an internal control. The primers and Taqman probe of β-actin were also added to the negative control to verify the absence of DNA contamination. Real-time PCR was conducted at 50°C for 2 minutes, then at 95°C for 10 minutes, followed by 40 cycles of 95°C for 15 seconds and 60°C for 1 minute. The relative level of epiplakin and involucrin transcripts were calculated as $2^{-\Delta Ct}$, where ΔCt=[Ct of target gene – Ct of actin gene]. The experiments were performed at least three times, each with triplicate samples.

RNA interference and establishment of stable cell lines

Epiplakin was knocked down by siRNA with the target sequence of 5′-AAGATGAGCATCTACCAGGCC (siRNA-KD: duplex RNA of epiplakin target sequences) which is located in the last six copies of the B domain of human epiplakin (AB051895). For the negative control, the scrambled target sequence of 5′-AAGTATACAGC-CCGCTAGCAG (siRNA-SC: duplex RNA of scrambled epiplakin target sequences) was used. Both double-stranded RNAs were obtained through in vitro transcription by using the Silencer siRNA Construction Kit (Ambion). For transient transfection, the indicated

concentration of siRNA-KD was transfected into cells by lipofectamin 2000 (Invitrogen). As for the control, cells were also transfected with siRNA-SC or exposed to lipofectamin 2000 alone. The level of epiplakin was monitored at 48-72 hours post-transfection.

To establish the epiplakin stable knockdown cell lines, DNA oligos of the target sequence or the scrambled sequence were cloned into pSilencer (Ambion) to obtain pSilent/Epi-KD and pSilent/Epi-SC constructs. HeLa cells were transfected with indicated plasmids (4 μg) using Fugene 6 (Roche) as described previously (Jang and Steinert, 2002). One day after transfection, cells were split in a 1:3 ratio under the selection medium containing 0.2 mg/ml hygromycin B (Invitrogen). The cultures were maintained with selection for 2 weeks, the hygromycin B-resistant colonies were isolated and transferred to 24-well plates. A total of 20 clones from each construct were selected and screened by immunofluorescent staining and western blotting. The positive clones (2 from each plasmid) were expanded and maintained in the growth medium containing hygromycin B. The establishments of stable HeLa cell lines were repeated twice.

Co-transfection and rescue experiments

To study the effects of the epiplakin linker, B domain and their combination on IF networks in the absence of endogenous epiplakin, pEGFP-epiplakin constructs were used in conjunction with RNAi study. Since B13 domain cDNA contains the target sequences of siRNA, three silent mutations (lower case letters, AAGATGAGtATaTAtCAGGCC) were generated in pEGFP-B13 and pEGFP-L12B13 constructs. These were made to prevent the knock down by siRNA-KD on the mRNA derived from the expression of pEGFP-B13 and pEGFP-L12B13 constructs. HeLa cells were seeded in a 4-well chamber slide (15,000 cells/chamber) 1 day before transfection. The indicated pEGFP-epiplakin constructs (200 ng) were either co-transfected with siRNA-KD (50 nM) into wild-type HeLa cells (for prevention experiments) or transfected into the stable epiplakin knockdown cell lines established by pSilent/Epi-KD (for rescue experiments). The cultures were fixed 48 hours post-transfection and processed for immunofluorescent staining as described above.

Results

The presence and distribution of epiplakin in cultured cells

Although the expression of epiplakin in various tissues has been reported (Fujiwara et al., 2001), the subcellular localization of human epiplakin in cultured epithelial and epidermal cells remained unclear. We first obtained a polyclonal antibody against a peptide sequence found in each of the last five linker domains. The specificity of the epiplakin antibody was evaluated by immunoblot analysis whereby only one band with high molecular mass was observed in NHEK-L but not in Cos7 cells (Fig. 1A). However, when a lower percentage of polyacrylamide gel and less secondary antibody were used, the epiplakin antibody recognized two bands in different cell lines (Fig. 1B). These bands were found in both soluble and insoluble fractions of NHEK-L and HeLa cells. However, the doublet was detected only in the soluble faction of HaCaT cells. These bands also showed different apparent molecular masses in different types of cells. Of note, the precise molecular mass of each band could not be determined since it is known that plakin proteins run aberrantly in SDS-PAGE gel (Stappenbeck et al., 1993). Nevertheless, using the rabbit skeletal myofibril, which contained titin, nebulin and myosin as reference markers, we estimated that the sizes of human epiplakin ranged from 510 kDa in NHEK cells (lower band) to 750 kDa in HaCaT cells (higher band). Since epiplakin is encoded by a single exon (Takeo et al., 2003), it is probable that these bands might result from the post-translation modification; however, the degradation of epiplakin during the preparation can not be ruled out.

As revealed by immunofluorescent staining (Fig. 1C), the distribution of epiplakin showed a filamentous pattern extending to the peripheral regions in the cytoplasm in HeLa, A431 and HaCaT. The pattern of epiplakin distribution was close to IF networks rather than microfilament or microtubule networks. Interestingly, epiplakin staining showed a diffuse pattern in NHEK-L cells, but with some thin filamentous structures (Fig. 1C, arrows in d). Additionally, not all keratinocytes stained positively for epiplakin. Only the large cells, which were

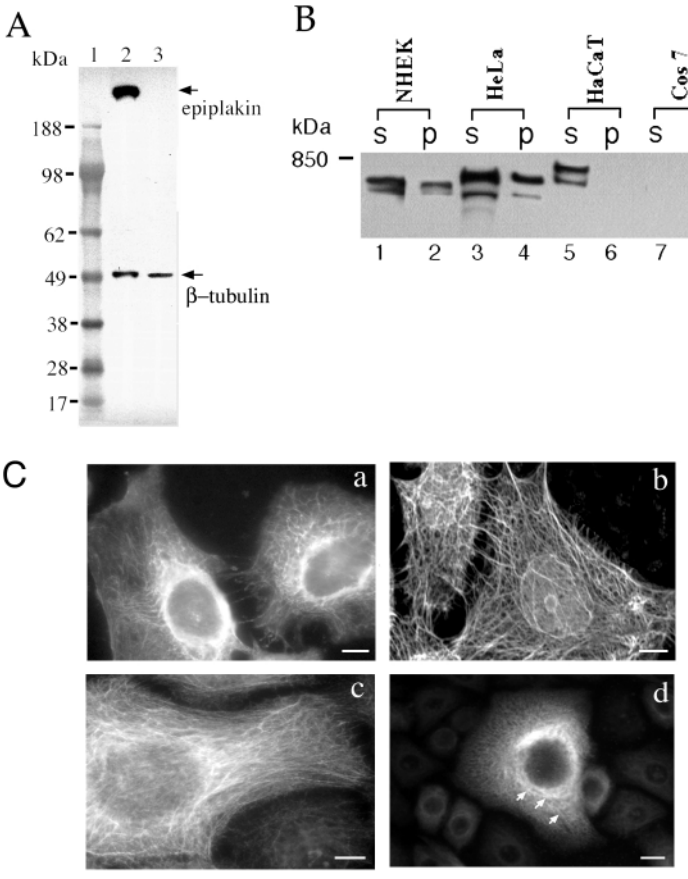

Fig. 1. Immunoblotting analyses and the distribution of epiplakin in cultured cells. (A) Immunoblot of NHEK-L (lane 2) and Cos-7 (lane 3) extracts probed with an antibody to epiplakin. β-tubulin is shown as a loading control. (B) Equal amounts of the soluble (S) and insoluble (P) fractions were resolved in a 3% SDS-NuPAGE gel and transferred to PVDF membrane, probed with the anti-epiplakin (1:2000) and the HRP-conjugated anti-rabbit antibodies (1:20,000). Nebulin, with a molecular mass of 850 kDa, is marked.
(C) Immunofluorescent staining of HeLa (a), A431 (b), HaCaT (c) and NHEK-L (d) cells. Cells were fixed in cold methanol and stained with anti-epiplakin antibody. The thin filament structure is indicated by arrows in d. Bars, 20 μm.

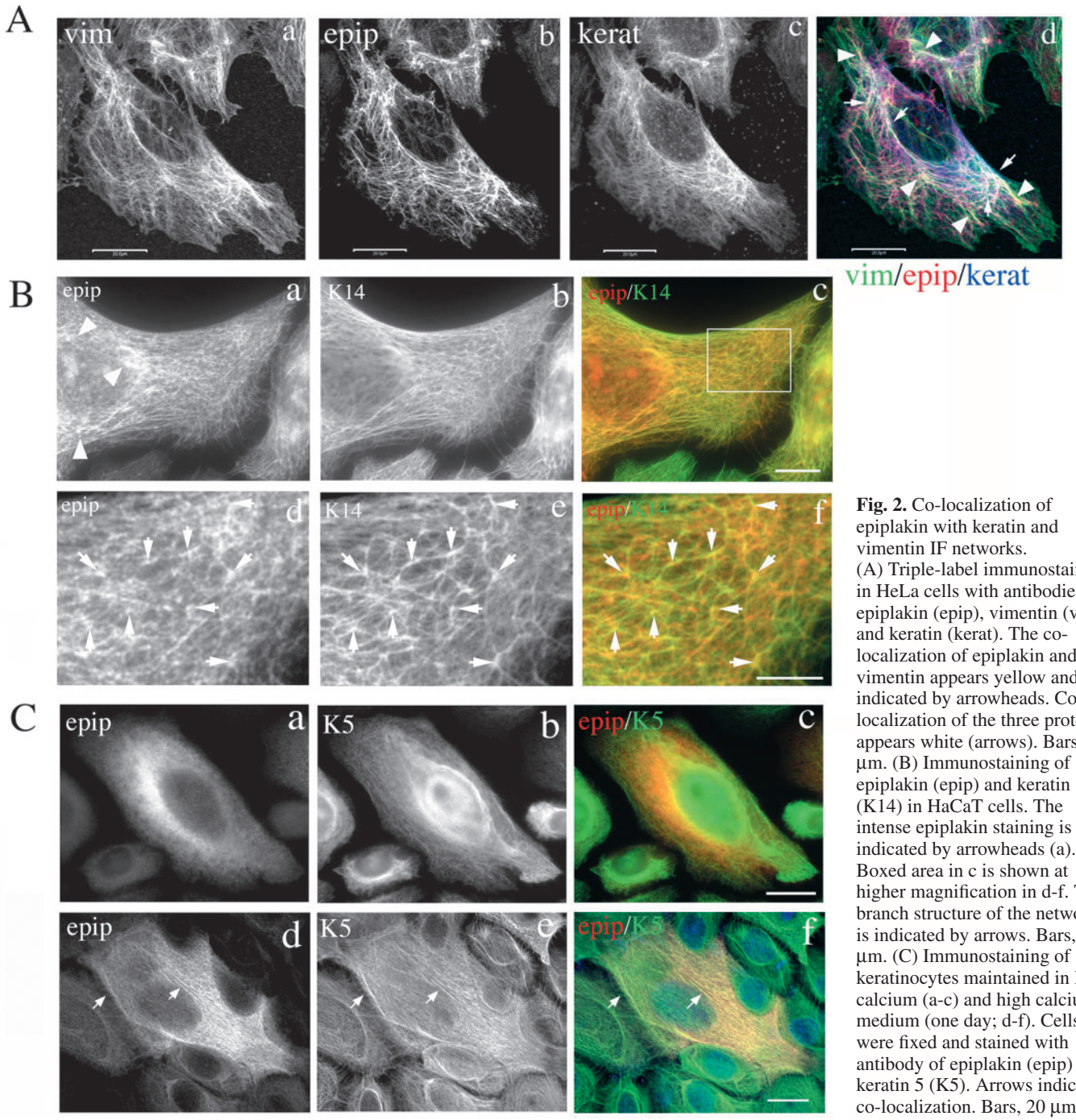

Fig. 2. Co-localization of epiplakin with keratin and vimentin IF networks. (A) Triple-label immunostaining in HeLa cells with antibodies to epiplakin (epip), vimentin (vim) and keratin (kerat). The co-localization of epiplakin and vimentin appears yellow and is indicated by arrowheads. Co-localization of the three proteins appears white (arrows). Bars, 20 μm. (B) Immunostaining of epiplakin (epip) and keratin 14 (K14) in HaCaT cells. The intense epiplakin staining is indicated by arrowheads (a). Boxed area in c is shown at higher magnification in d-f. The branch structure of the network is indicated by arrows. Bars, 10 μm. (C) Immunostaining of keratinocytes maintained in low calcium (a-c) and high calcium medium (one day; d-f). Cells were fixed and stained with antibody of epiplakin (epip) and keratin 5 (K5). Arrows indicate co-localization. Bars, 20 μm.

undergoing terminal differentiation, expressed epiplakin, suggesting that the expression might be regulated in differentiating keratinocytes. This is further supported by the observation that more keratinocytes showed positive epiplakin staining with an obvious filamentous pattern in NHEK cultures after the calcium switch (see below).

Co-localization of epiplakin and IF networks

The association of plakins and cytoskeleton has been well documented (for a review, see Leung et al., 2002). With the decoration of the IF network by epiplakin, we next examined the co-localization of epiplakin and cytoskeletal networks. To have a better comparison of the distribution of epiplakin, keratin and vimentin, a triple-color staining was performed in HeLa cells (Fig. 2A). Although all three proteins showed a filamentous pattern, the staining of epiplakin co-localized more closely with keratin (pinkish color in Fig. 2A,d) than with vimentin throughout the cytoplasm. Epiplakin localized with vimentin in some places with thick filament structures in the cytoplasm (yellow, arrowheads in Fig. 2A,d). In some areas, the thick filament structures appear white indicating that all three proteins co-localized (arrows in Fig. 2A,d). The co-localization between epiplakin and epidermal keratin IF was

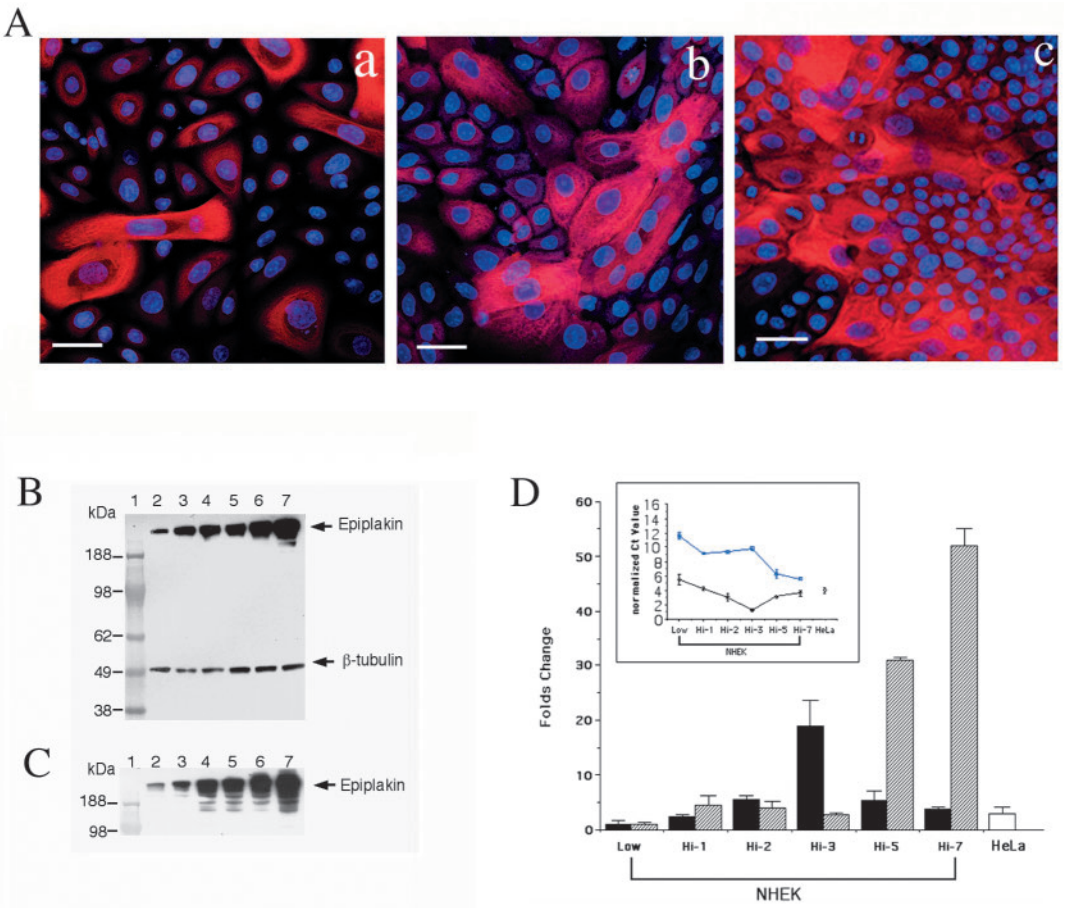

Fig. 3. Up-regulation of epiplakin expression in keratinocytes. (A) Immunofluorescent staining of NHEK cells maintained in low calcium (a) and high calcium for 1 day (b) or high calcium for 3 days (c), fixed and stained with anti-epiplakin (red) antibody and TO-PRO 3 for nuclei (blue). Bars, 20 μm. (B,C) Immunoblotting of soluble (B) and insoluble (C) fractions from NHEK-L (lane 2) or NHEK-H of 1 (lane 3), 3 (lane 4), 5 (lane 5), 7 (lane 6) and 9 days (lane 7) were probed with epiplakin antibody. β-tubulin is shown as a loading control. (D) Real-time RT-PCR analysis of epiplakin and involucrin transcripts in NHEK cells. The threshold values (Ct) of epiplakin and involucrin were normalized by the subtraction of the Ct value of β-actin in each corresponding samples (insert: epiplakin, black line; involucrin, blue line). Three separate experiments were performed with triplicate samples. The data are presented as a fold change (mean ± s.d.) of the relative level of epiplakin (black and white bars) and involucrin (hatched bar) from NHEK-H or HeLa over that of NHEK-L sample.

also found in HaCaT cells (Fig. 2B). Epiplakin co-aligns with K14 throughout the cytoplasm and peripheral regions. In some branch regions, a strong co-localization signal was observed (arrows in Fig. 2B,d-f). However, epiplakin showed more intensive staining especially around the perinuclear region (arrowheads in Fig. 2B,a). Also, epiplakin staining was not as even and clear a filamentous pattern, as the K14 staining. This might be because of the different affinity of the antibody used.

In contrast to the HeLa cells, almost all of which expressed epiplakin, not all the NHEK cells showed positive staining of epiplakin (Fig. 1C). In large keratinocytes, epiplakin staining was diffuse and it did not co-align with K5 in NHEK-L cells (Fig. 2C,a-c). However, one day after the calcium-switch, more keratinocytes showed positive staining with an obvious filamentous pattern that was clearly co-aligned with K5 (Fig. 2C, arrows in d-f). These observations suggest the potential involvement of the calcium elevation in the expression and organization of epiplakin in NHEK cells.

Expression of epiplakin is up-regulated in differentiating keratinocytes

Until recently, only two plakins, envoplakin and periplakin, were reported as being up-regulated in differentiating keratinocytes (Ruhrberg et al., 1996; Ruhrberg et al., 1997). The immunofluorescent staining of epiplakin in NHEK cells revealed that the epiplakin level increased after the calcium switch. We conducted a time-course study to monitor the level of epiplakin in differentiating keratinocytes. As shown in Fig. 3A, the population of keratinocytes with positive epiplakin staining increased from 10% in low calcium medium to more than 80% in 3 days under the high calcium condition. The increase of epiplakin expression was further confirmed by immunoblotting analysis in which the level of epiplakin increased with time, in both soluble (Fig. 3B) and insoluble (Fig. 3C) fractions. Epiplakin increased by more than tenfold in NHEK-H at day 9 of culture (lane 7) compared to the NHEK-L cells sample (lane 2) in both fractions. Furthermore, multiple bands with lower molecular masses appeared in insoluble fractions after day 3 (lanes 4-7), suggesting possible processing of epiplakin in terminally differentiating keratinocytes.

Next, we examined whether the increase in epiplakin in NHEK resulted from up-regulation at the transcriptional level. By using real-time RT-PCR it was determined that the level of β-actin transcript remained constant throughout the course of study and it was used as an internal control (data not shown). The relative level of the epiplakin transcript showed a 2.5-fold increase one day after the calcium switch (Fig. 3D, black bars). The increase continued up to day 3 at which time the transcript was more than 15-fold higher than in NHEK-L cultures. At this point, the abundance of epiplakin transcript was equivalent to half that of the β-actin transcript (Fig. 3D, insert, black line).

The level of epiplakin transcript then decreased in day 5 and day 7 cultures to about fivefold and fourfold over the control, respectively. However, epiplakin protein continued to accumulate during the same period of time (Fig. 3B,C). In a parallel experiment, the level of epiplakin transcript in HeLa cells was measured (Fig. 3D, white bar), and it was equivalent to that of one-day NHEK-H cultures. As for the control to monitor the keratinocyte differentiation, the level of involucrin transcript increased substantially after day 3 of high calcium (Fig. 3D, hatched bars). These data demonstrate that the increase of epiplakin expression in differentiating keratinocytes indeed resulted from up-regulation at the transcriptional level. We did not further examine the role of epiplakin in keratinocyte differentiation since it was beyond the scope of the current study.

The repeat unit (linker plus PRD) of epiplakin preferentially associates with assembled keratin filaments

The filamentous pattern of epiplakin staining in cultured cells raised the possibility of interaction between epiplakin and IFs. Since epiplakin comprises multiple copies of linker and B domains (Fig. 4A), the dot blot overlay assays were conducted to determine if the linker and/or the B repeat domains were essential for the interaction. Owing to the enormous size and highly repetitive nature of human epiplakin, we failed to obtain the full length human epiplakin cDNA by conventional PCR. However, since the last five to eight copies of repeated domains (linker and B repeat domains) are virtually identical, we turned our attention to the last region of the linker (L12) and B repeat (B13) in which their combinations were fused with GST protein (see Table 1). As shown in Fig. 4B, GST-EpiB13 showed modest binding with vimentin, K5, K8 and assembled K8/K18 filament, and weak binding with K14 and assembled K5/K14 filament, but no association with involucrin and K18. The linker alone (GST-EpiL12) did not associate with any proteins except vimentin which showed weak, but detectable binding. In contrast, the combination of linker and B repeat domains (GST-EpiL12B13) showed strong association with vimentin, K14, K5/K14 filament and K8/K18 filament, whereas modest binding was observed with K18 monomer. Furthermore, GST-EpiL12B13 interacted preferentially with assembled filaments rather than keratin monomers. This is particularly evident in the case of simple epithelial keratin IF, where a much stronger interaction with K8/K18 IF was observed than with K18 or K8 monomers. These data demonstrate that both linker and B domain of epiplakin are necessary for the association with keratin and vimentin IF in vitro.

Knock down of epiplakin results in disarray of IF networks in HeLa cells

The data presented so far suggest that epiplakin might function as an IF-associated protein. To further understand the biological role of epiplakin, an RNAi experiment was conducted to deplete the endogenous epiplakin. The effective target sequences for epiplakin knockdown were determined empirically. To monitor the transfection efficiency of siRNA-KD duplex, the transiently transfected HeLa cells were first monitored by immunofluorescence analysis. As shown in Fig. 5A, more than 90% of the cells did not show epiplakin staining compared with the control transfected with siRNA-SC duplex.

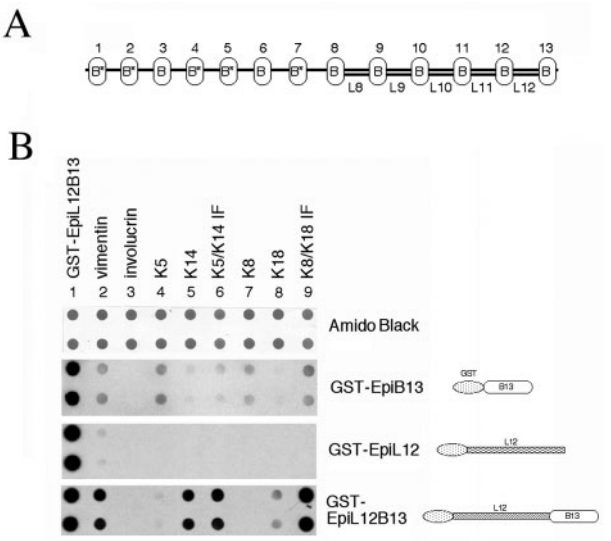

Fig. 4. Overlay binding assay of epiplakin fragments with vimentin, keratins and assembled IFs. (A) Schematic illustration of human epiplakin 9 [according to the nomenclature of Fujiwara et al. (Fujiwara et al., 2001)]. (B) Dot-blot binding assay of recombinant purified monomeric or polymerized IF proteins with expressed epiplakin fragments (right: schematic representation of the GST-fused epiplakin constructs). The indicated recombinant proteins were spotted in duplicate onto three membranes as described in Materials and Methods. The expressed GST-EpiL12B13 protein (lane 1) served as a positive control for GST antibody. Protein loading was monitored by Amido Black staining. The experiments were repeated in at least three times and one representative set of data is shown.

This was further confirmed by western blotting where the endogenous epiplakin was dose-dependently knocked down by siRNA-KD duplex in HeLa cells (Fig. 5B). Transfection of 2 nM and 50 nM siRNA-KD duplex caused 40% and 90% reduction compared to the control, respectively.

The effects of epiplakin depletion on cytoskeleton structures were then studied in HeLa cells. If epiplakin interacts with vimentin and keratins in vitro as demonstrated in the binding assays, lowering its level should affect the IF networks. As predicted, the phenotypic analyses using the triple-color staining showed that disorganized keratin and vimentin IF networks with a focal concentration at the perinuclear region were present in transfected cells that had faint epiplakin staining (Fig. 5C). By contrast, the IF networks of keratin and vimentin remained intact in the non-transfected cells where abundant epiplakin with a filamentous pattern was observed (arrows in Fig. 5C,a-d). These results showed that epiplakin plays an important role in the integrity of both IF networks in epithelial cells. We also found that the absence of epiplakin did not affect microfilament (Fig. 5C,f) or microtubule networks (data not shown). The RNAi experiments were also performed in HaCaT and NHEK cells. Compared with the control, epiplakin was also effectively reduced by the siRNA-KD duplex in NHEK cells maintained either in low or high calcium condition (Fig. 6A). However, we did not see any disruption of epidermal keratin IF networks in either case (data not shown). Similar results were observed in HaCaT cells where epiplakin was significantly depleted by RNAi (Fig. 6B), yet the keratin IF network remained intact. These results demonstrate that

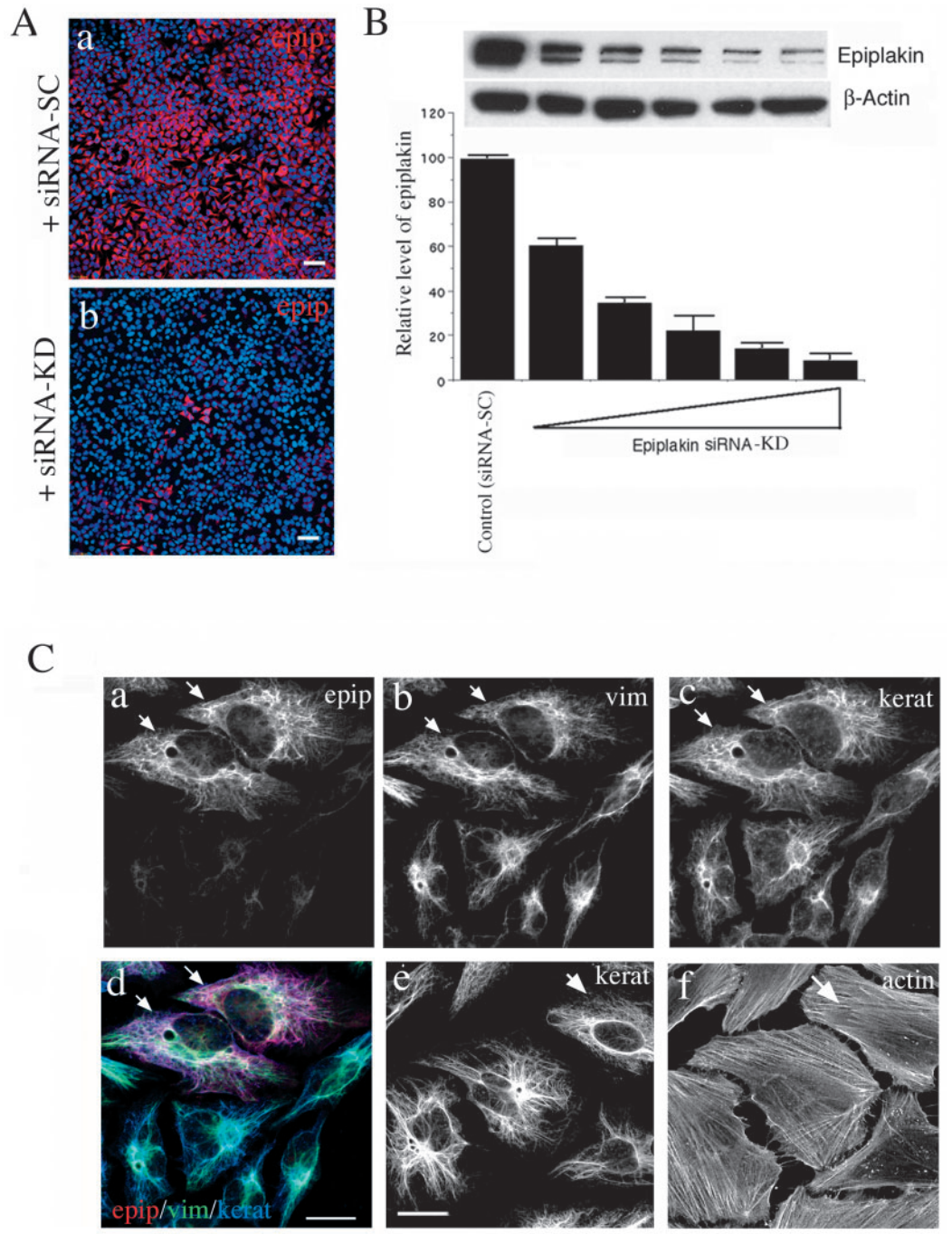

Fig. 5. Knock down of epiplakin by RNAi. (A) Immunostaining of HeLa cells transiently transfected with siRNA-SC (a) and siRNA-KD (b). Cells were fixed and stained with the anti-epiplakin (epip) antibody. Nuclei were stained with TO-PRO 3 (blue). Bars, 30 μm. (B) Western blotting analysis of epiplakin expression in HeLa cells transiently transfected with siRNA-SC or siRNA-KD (2, 5, 10, 25, and 50 nM). Cellular extracts were fractionated on a 3% SDS-NuPAGE gel and probed with anti-epiplakin antibody. β-actin is shown as a loading control. The level of epiplakin was measured by densitometry and normalized to β-actin in each corresponding sample. The data (mean ± s.d.) are averages from three separate experiments with duplicate samples and are presented as a fold change from the sample of siRNA-KD over that of siRNA-SC. (C) Immunostaining analysis of HeLa cells transiently transfected with siRNA-KD. (a-d) Cells were subjected to triple-label staining with the antibodies specific for epiplakin, vimentin and keratin. (e,f) In a parallel experiment, cells were double-stained with antibodies for keratin (kerat) and β-actin (actin). The non-transfected cells are indicated by arrows (a-f). Bars, 20 μm.

epiplakin plays a more critical role in maintaining the IF networks in simple epithelial cells than in epidermal cells.

It has been reported that the transient effect of knockdown lasts only for 4-7 days (Tijsterman et al., 2002). To further study the long-term consequences of epiplakin depletion, stable HeLa cell lines were established by expressing siRNA-KD duplex driven by a human U6 promoter for continuous knockdown of epiplakin. Western blotting showed that only a trace amount of epiplakin was found in two clones transfected with the pSilent/Epi-KD construct compared to the control transfected with pSilent/Epi-SC construct (Fig. 7A). Consistent with the results from the transient knockdown study, the cells with the stable epiplakin knockdown showed faint epiplakin staining with disorganized keratin (Fig. 7B,c,f) and vimentin (see below) IF networks, whereas the microfilament and microtubulin networks remained intact (Fig. 7B,b,e). The control stable cell lines showed the normal filamentous pattern of epiplakin, keratin and vimentin (Fig. 7B,g-i). These results demonstrate that epiplakin is critical for the integrity of IF networks in simple epithelial cells.

The repeat unit of epiplakin is able to prevent the collapse of IF networks and partially restore the keratin IF network in HeLa cells

The fragments of epiplakin showed different preferences in

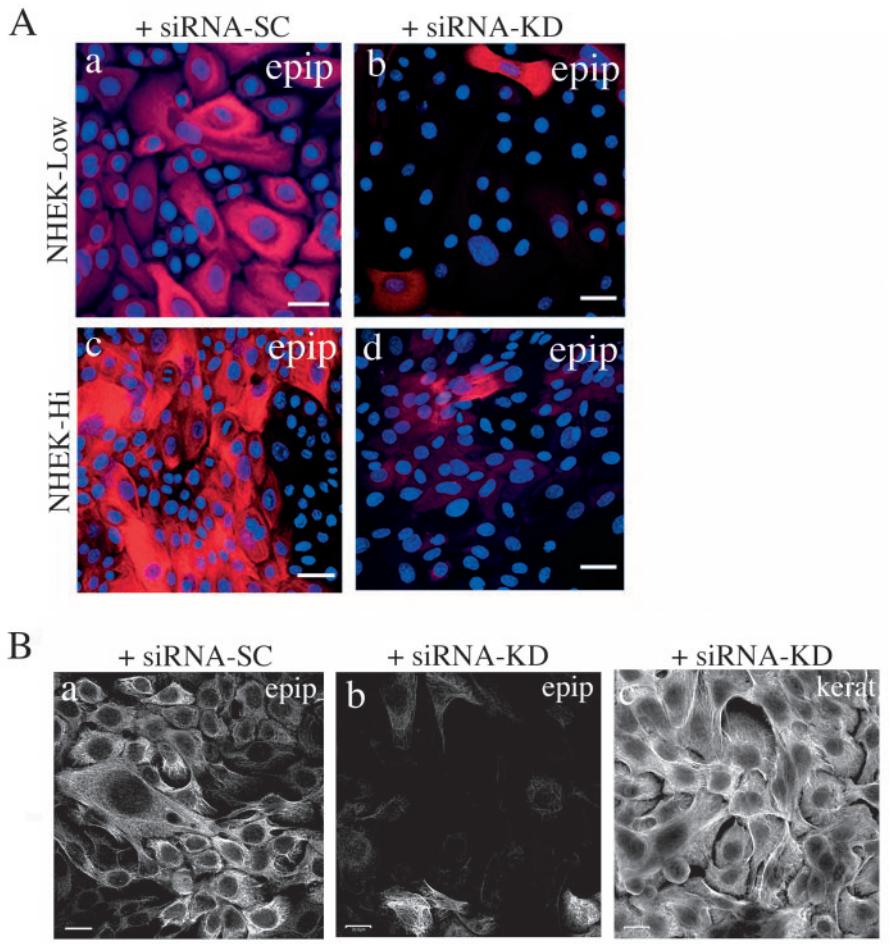

Fig. 6. The knock down of epiplakin in epidermal cells. (A) Immunofluorescent staining of epiplakin in NHEK transiently transfected with the indicated RNA duplex and maintained in either low calcium (NHEK-Low; a,b) or high calcium (NHEK-Hi; c,d) medium for 2 days, fixed and stained with anti-epiplakin antibody (red). Nuclei were stained with TO-PRO 3 (blue). Bars, 20 μm. (B) Immunofluorescent staining in HaCaT cells transiently transfected with 50 nM of siRNA-SC (a) or siRNA-KD (b,c) were stained with anti-epiplakin (epip; a,b) and anti-keratin (kerat; c). b and c are from the same field. Bars, 20 μm.

association with vimentin and the keratins in vitro (Fig. 4B). In an attempt to further study the effects of these fragments on IF networks in the absence of endogenous epiplakin in vivo, the pEGFP-fused constructs were used in conjunction with the RNAi experiments. Since the target sequence of RNAi was located on the B13 domain, three silent mutations were made to avoid the knockdown on the transcripts derived from pEGFP-B13 and pEGFP-L12B13 constructs. In the transient knockdown rescue experiments, we first co-transfected the pEGFP-fused epiplakin constructs together with siRNA-KD into HeLa cells and evaluated the IF networks by immunostaining. As shown in Fig. 8A, the expression of the B13 domain was in an aggregate formation around the perinuclear region (Fig. 8A,a). The linker itself (L12, Fig. 8A,d) showed punctate distribution in the cytoplasm and peripheral regions. Furthermore, both vimentin and keratin IF networks remained disorganized in the cells transfected with either pEGFP-B13 (Fig. 8A,b,c) or pEGFP-L12 (Fig. 8A,e,f) construct. In contrast, transfection of the pEGFP-L12B13 construct resulted in both fine and thick filament structures (Fig. 8A,g). Furthermore, compared to the non-transfected cells, both vimentin and keratin IF networks remained intact in the transfected cells (Fig. 8Ah,i). These observations not only support the results from the dot blot assays on the association of the L12B13 fragment with vimentin and assembled keratin IFs, but also demonstrates functionally that the repeat unit of the L12B13 fragment, when introduced together with siRNA-KD, is sufficient to prevent the disruption of vimentin and keratin IF networks in HeLa cells.

To further confirm these observations, we conducted stable knockdown rescue experiments. The EGFP-fused epiplakin constructs were transfected into the stable epiplakin knockdown HeLa cell lines. These cells retained the intact microfilament and microtubule networks but contained disorganized IF networks (Fig. 7B). Consistent with the results from transient co-transfection experiments, the IF networks remained disarrayed in the cells transfected with either pEGFP-B13 or pEGFP-L12 constructs (data not shown). In the case of pEGFP-L12B13 transfection, the keratin filament network did not show a disorganized pattern, unlike the non-transfected cells, which the keratin network was in disarray (Fig. 8B,c). However, both epiplakin and keratin staining (Fig. 8B,b,c) did not display an obvious filamentous pattern compared to the observations from transient transfection (Fig. 8A,i). In addition, the vimentin IF network remained disorganized regardless of the presence of the L12B13 fragment (Fig. 8B,f). These results demonstrate that the L12B13 fragment was able to partially restore the collapsed keratin but not vimentin IF network in these stably knocked down HeLa cell lines.

Discussion

Until recently, only a few studies on epiplakin had been reported, and little is known about its role in epithelial cells. We speculated that epiplakin, as a member of the plakin family, might function as a cytolinker involved in the cytoskeletal infrastructures in epithelial tissues. It has been shown that the PRD of plakins is important in mediating IF binding. Unlike other conventional plakins, epiplakin contains only multiple copies of PRD together with various sizes of linkers. It is worthwhile noting that the linker of epiplakin is quite different from the conserved linker (L subdomain), which is located downstream of the B subdomain of desmoplakin and plectin. Epiplakin has different sizes of linker, especially the last five linkers (356 residues, L8-L12, Fig. 6A), which are twice the size of the associated B domain and are conserved only within epiplakin itself. By using part of the linker sequences as an

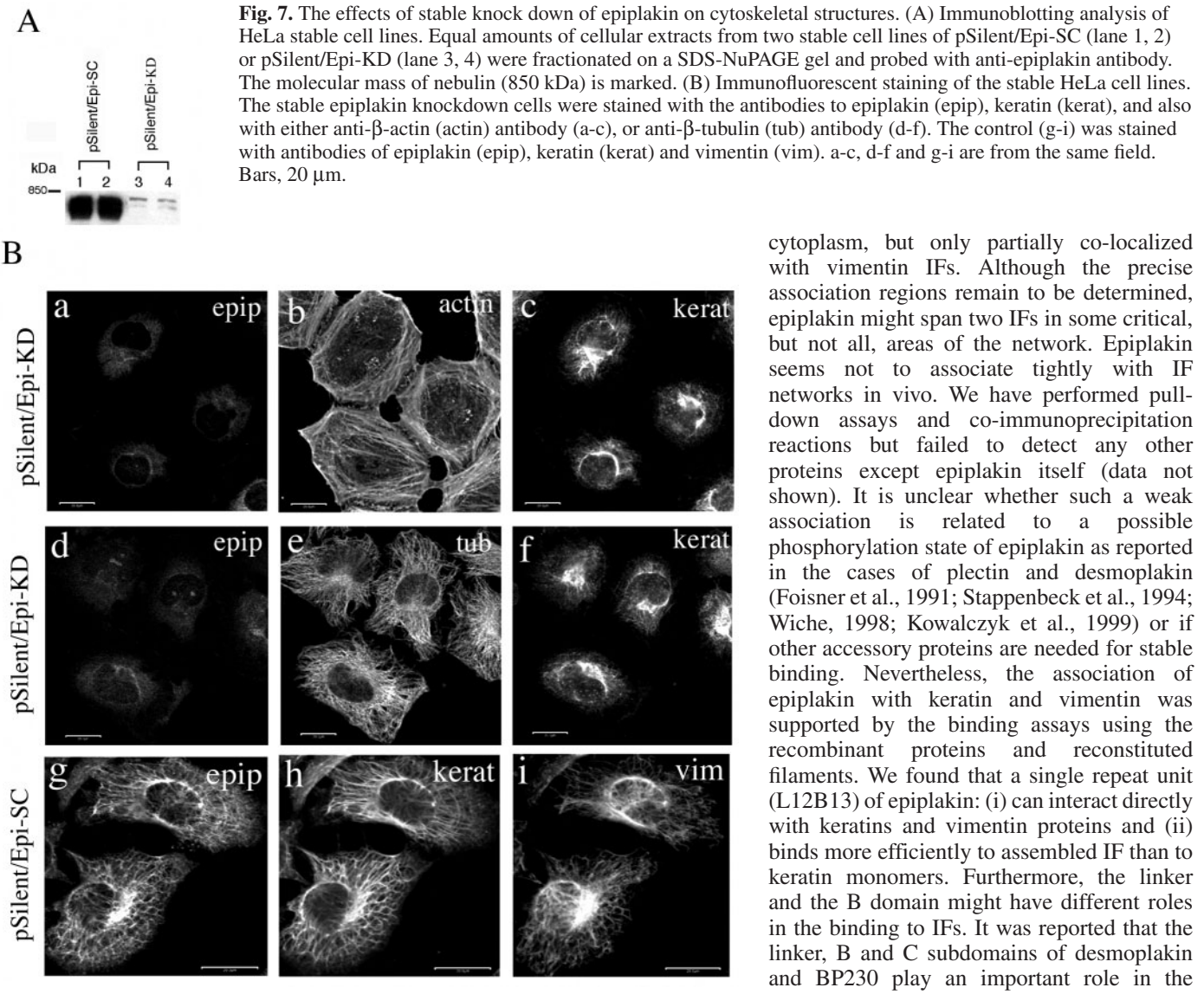

Fig. 7. The effects of stable knock down of epiplakin on cytoskeletal structures. (A) Immunoblotting analysis of HeLa stable cell lines. Equal amounts of cellular extracts from two stable cell lines of pSilent/Epi-SC (lane 1, 2) or pSilent/Epi-KD (lane 3, 4) were fractionated on a SDS-NuPAGE gel and probed with anti-epiplakin antibody. The molecular mass of nebulin (850 kDa) is marked. (B) Immunofluorescent staining of the stable HeLa cell lines. The stable epiplakin knockdown cells were stained with the antibodies to epiplakin (epip), keratin (kerat), and also with either anti-β-actin (actin) antibody (a-c), or anti-β-tubulin (tub) antibody (d-f). The control (g-i) was stained with antibodies of epiplakin (epip), keratin (kerat) and vimentin (vim). a-c, d-f and g-i are from the same field. Bars, 20 μm.

epitope, the epiplakin antibody recognized two bands in both epithelial and epidermal cells. It is unlikely that these resulted from alternative splicing, since it is encoded by a single exon. It is possible that these bands resulted from post-translation modification. In addition, the molecular mass of human epiplakin was 725 kDa in HaCaT cells, similar to mouse epiplakin (Spazierer et al., 2003). This is different from the estimated 552 kDa in HeLa cells, reported by Fujiwara et al. (Fujiwara et al., 2001). Our data showed that the size of human epiplakin could vary from 510 to 750 kDa depending upon the cell types. It is not yet clear why different sizes of epiplakin were found in different cell types. We speculate that human epiplakin might have a different start codon present or it might be processed post-translationally into different sizes in different cell types; however, this remains to be clarified.

Epiplakin decorates IF networks in both epithelial and epidermal cultured cells. This is in agreement with the recent report on mouse epiplakin which was shown to have a partly filamentous structure in hepatocytes (Spazierer et al., 2003). Based on the triple-label staining, the filamentous pattern of epiplakin was well localized with keratin IFs throughout the cytoplasm, but only partially co-localized with vimentin IFs. Although the precise association regions remain to be determined, epiplakin might span two IFs in some critical, but not all, areas of the network. Epiplakin seems not to associate tightly with IF networks in vivo. We have performed pull-down assays and co-immunoprecipitation reactions but failed to detect any other proteins except epiplakin itself (data not shown). It is unclear whether such a weak association is related to a possible phosphorylation state of epiplakin as reported in the cases of plectin and desmoplakin (Foisner et al., 1991; Stappenbeck et al., 1994; Wiche, 1998; Kowalczyk et al., 1999) or if other accessory proteins are needed for stable binding. Nevertheless, the association of epiplakin with keratin and vimentin was supported by the binding assays using the recombinant proteins and reconstituted filaments. We found that a single repeat unit (L12B13) of epiplakin: (i) can interact directly with keratins and vimentin proteins and (ii) binds more efficiently to assembled IF than to keratin monomers. Furthermore, the linker and the B domain might have different roles in the binding to IFs. It was reported that the linker, B and C subdomains of desmoplakin and BP230 play an important role in the specificity and interaction with IFs (Fontao et al., 2003). We observed preferential binding of epiplakin fragments to different type of keratins. In the case of the B domain alone, it favored binding with type II over type I keratins. This is similar to desmoplakin, which associates preferentially with type II epidermal keratins (Meng et al., 1997). However, opposite results were observed when both linker and the B domain were present, indicating that the linker affects the binding preference of B domain. The linker might enhance the binding to vimentin and assembled keratin IFs since the linker alone did not show any binding and the B

Table 2. The effects of epiplakin knock-down on cytoskeletal structures

Cell type	Microfilament network	Microtubule network	Intermediate filament network
Simple epithelial cell line: HeLa	–	–	+
Epidermal cell line: HaCaT	–	–	–
Primary keratinocytes: NHEK	–	–	–

–, network remains intact; +, network collapse.

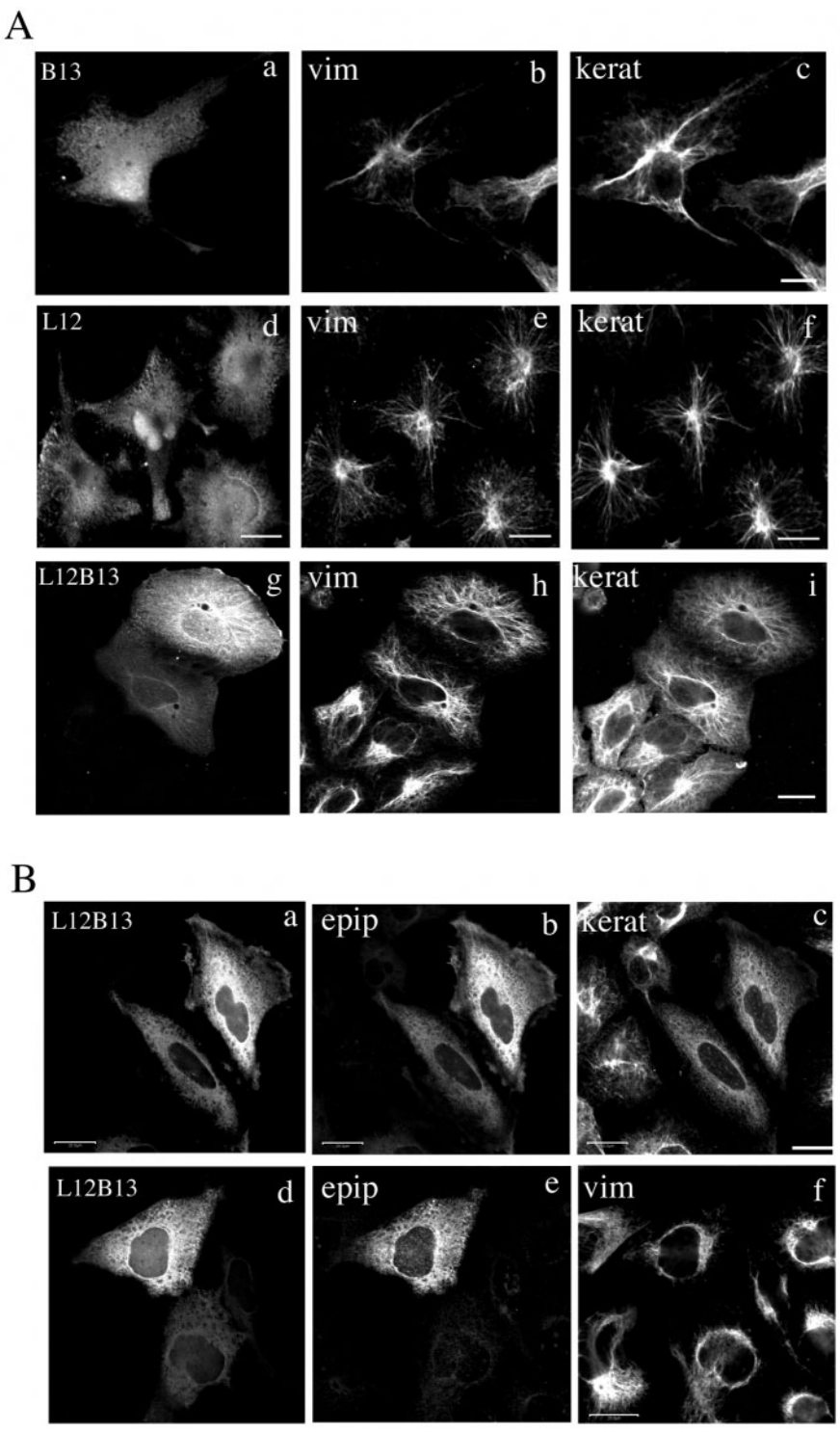

Fig. 8. The effects of epiplakin linker and B domain on the IF network in the absence of epiplakin. (A) Immunofluorescence analysis of HeLa cells transiently transfected with siRNA-KD together with pEGFP-B13 (a-c), pEGFP-L12 (d-f) or pEGFP-L12B13 (g-i). Cells were fixed and double-stained with anti-vimentin (vim; b,e,h) and anti-keratin (kerat; c,f,i) antibodies. a, d and g show the green fluorescence signal of EGFP. Panels a-c, d-f and g-i are from the same field. Bars, 20 μm. (B) Immunofluorescence analysis of stable epiplakin knockdown HeLa cell lines. Cells were transiently transfected with pEGFP-L12B13 and were double-stained with anti-epiplakin (epip; b,e), anti-keratin (kerat; c) or anti-vimentin (vim; f) antibodies. a and d show the green fluorescence signal of EGFP. a-c and d-f are from the same field. Bars, 20 μm.

domain itself showed only modest or weak association. Furthermore, the expression of the EGFP-fused L12B13 fragment was seen as a filamentous structure in both thin and thick patterns when epiplakin was knocked down (Fig. 8A). This supports the results of the overlay binding assays which showed that the repeat unit (L12B13) was sufficient for a robust binding to vimentin and assembled keratin IFs.

In contrast to the absence of a filamentous pattern in mouse keratinocytes as reported by Spazierer et al. (Spazierer et al., 2003), human epiplakin showed a fine, patchy filamentous pattern in NHEK-L cells and became more apparent in thicker filaments in NHEK-H cells. Similar to periplakin and envoplakin, the expression of epiplakin was up-regulated at the transcriptional level after the calcium switch. The relative level of the epiplakin transcript when it reached a peak during day 3 in NHEK-H cells was estimated to be about sixfold higher than in HeLa cells (Fig. 3D). It is unclear why epiplakin is expressed at such a high level, and what physiological roles epiplakin may play during the keratinocyte differentiation. We reason that if epiplakin acts as a bundling protein on IF networks, more epiplakin may be needed during the keratinocyte differentiation when another set of epidermal keratins K1/K10 starts to express. We also studied the involvement of epiplakin in the formation of the CE complexes and no epiplakin peptides were detected in CE isolated from a foreskin sample (data not shown). However, a recent study reported that epiplakin crosslinks to trichohyalin, keratin, SPR and involucrin in the inner root sheath of hair follicles (Steinert et al., 2003).

Gene ablation of several plakins has been well documented (reviewed by Leung et al., 2002). Based on the findings in this study, it will be interesting to see what the consequence of epiplakin knockout in mice will be. However, given the size and the highly repeated regions of the mouse epiplakin gene, it will be a challenge to generate the null mice of epiplakin. We have applied RNAi to effectively knock down human epiplakin in both epithelial and epidermal cells. To our surprise, the knockdown of epiplakin revealed quite different consequences in simple epithelial and epidermal cells (see Table 2). In simple epithelial cells, when epiplakin was knocked down, both keratin and vimentin IFs collapsed, suggesting that epiplakin might serve as a stabilizer for the integrity of IF networks. The depletion of epiplakin did not

seem to cause the collapse of IF networks immediately. We have observed that when HeLa cultures were treated with Triton X-100 prior to fixation, no epiplakin staining was found, yet both keratin and vimentin IF networks remained intact (our unpublished observation). This suggests that both existing IF networks could be sustained for a period of time after epiplakin was depleted. Another line of evidence to support this, as demonstrated in the transient knockdown rescue experiments, is that the expression of a copy of the repeat unit (L12B13) was able to prevent the collapse of both keratin and vimentin IF networks. Although the nature of the interaction is unclear, the presence of the overexpressed L12B13 domain could supplement the role of endogenous epiplakin as an IF-associated protein, and together with other unknown proteins maintain both keratin and vimentin IF networks. It should be noted that the L12B13 fragment can only represent the last five to eight repeats of epiplakin; whether the other copies of linker and B domain of epiplakin will have a role similar to the L12B13 repeat remains to be studied. In the stably knocked down rescue study, however, the L12B13 fragment could only partially restore the keratin network suggesting that these unknown proteins were no longer available for the full restoration of the keratin network. Furthermore, the collapse of the vimentin network most probably resulted from a secondary effect of the absence of epiplakin and the disorganized keratin IF network. This can be supported from two observations: (i) epiplakin only partially co-localized with vimentin on the thick filament structures (Fig. 2A), and (ii) the L12B13 fragment could not restore vimentin IF networks in the stably knocked down cell lines (Fig. 8B). The phenomenon of disorganized IF networks in the absence of epiplakin seems to be restricted only to simple epithelial cells. In epidermal cells, it is not clear why the absence of epiplakin did not have any effect on the structure of IF network in HaCaT and NHEK cells. We reason that epidermal cells contain more robust and complex keratin organization than simple epithelial cells. There may be other unidentified proteins that might have a compensatory role in preventing the collapse of the epidermal keratin IF network when epiplakin is depleted.

Despite the disarrayed IF networks, we observed that the stable knockdown HeLa cells continued to grow. We reason that since the actin and microtubule networks remained intact in these stable cell lines, the cells could survive through the support of microfilament and microtubule networks in the first few passages. However, these networks could not persist for a long period of time. The cells also became flat and large and could no longer withstand the mechanical stress during the passage that eventually led to cell rupture (our unpublished observation). The results of the current study and the fact that the expression of epiplakin is mainly restricted to epithelial tissues point to the important role of epiplakin for strengthening and/or maintaining the integrity of IF networks in these tissues to endure the mechanical stress. Therefore, in the case of epiplakin null mice, we speculate that there should have been some consequences in simple epithelia such as in esophagus, stomach and small intestine. However, it is still questionable whether the mice will show any skin phenotypes since the K5/K14 IF networks remained intact when epiplakin was knocked down in cultured keratinocytes. Also, the recent knockout studies on the key components of CE have demonstrated that involucrin, loricrin, envoplakin and periplakin are not crucial for CE formation and skin barrier function (Djian et al., 2000; Koch et al., 2000; Määttä et al., 2001; Aho et al., 2004).

Epiplakin in some ways behaves like other plakins in the decoration of IF networks in cytoplasm. However, unlike plectin, epiplakin does not appear to associate with microtubule or microfilament networks. Also, unlike periplakin or envoplakin, we do not have evidence that epiplakin is a component for CE formation in keratinocytes. In conclusion, we have characterized human epiplakin in cultured epithelial and epidermal cells. We shown that epiplakin functions as a cytolinker in association mostly with keratin and connects partially with vimentin IF networks. We have also demonstrated that epiplakin plays an important role in stabilizing/maintaining the IF networks in simple epithelial cells, and documented the increase of epiplakin transcript in differentiating keratinocytes. Further study on mapping the sequences responsible for the interaction for epiplakin and its partners should provide more insight into the role of epiplakin in epithelial cells.

Many thanks to Andrey Kalinin, David Perry, Evelyn Ralston, Alasdair Steven and Lisa Smith for their critical review and advice. We thank Kristien Zaal (light imaging section, NIAMS) for advice on confocal microscopy, Hui Zhao for help and suggestions on real-time RT-PCR and Gustavo Gutierrez-Cruz for the rabbit skeletal myofibril.

References

Aho, S., Li, K., Ryoo, Y., McGee, C., Ishida-Yamamoto, A., Uitto, J. and Klement, J. F. (2004). Periplakin gene targeting reveals a constituent of the cornified cell envelope dispensable for normal mouse development. *Mol. Cell. Biol*. **24**, 6410-6418.

Andrä, K., Lassmann, H., Bittner, R., Shorny, S., Fässler, R., Propst, F. and Wiche, G. (1997). Targeted inactivation of plectin reveals essential function in maintaining the integrity of skin, muscle, and heart cytoarchitecture. *Genes Dev.* **11**, 3143-3156.

Bernier, G., Mathieu, M., de Repentigny, Y., Vidal, S. M. and Kothary, R. (1996). Cloning and characterization of mouse ACF7, a novel member of the dystomin subfamily of actin binding proteins. *Genomics* **39**, 19-29.

Bornslaeger, E. A., Godsel, L. M., Corcoran, C. M., Park, J. K., Hatzfeid, M., Kowalczyk, A. P. and Green, K. J. (2001). Plakophilin 1 interferes with plakoglobin binding to desmoplakin, yet together with plakoglobin promotes clustering of desmosomal plaque complexes at cell-cell borders. *J. Cell Sci.* **114**, 727-738.

Borradori, L. and Sonnenberg, A. (1996). Hemidesmosomes: roles in adhesion, signaling and human diseases. *Curr. Opin. Cell Biol.* **8**, 647-656.

Brown, A., Bernier, G., Mathieu, M., Rossant, J. and Kothary, R. (1995). The mouse dystonia musculorum gene is a neural isoform of bullous pemphigoid antigen 1. *Nat. Genet.* **10**, 301-306.

Burgeson, R. E. and Christiano, A. M. (1997). The dermal-epidermal junction. *Curr. Opin. Cell Biol*. **9**, 651-658.

DiColandrea, T., Karashima, T., Määttä, A. and Watt, F. M. (2000). Subcellular distribution of envoplakin and periplakin, insights into their role as precursors of the epidermal cornified envelope. *J. Cell Biol.* **151**, 573-585.

Djian, P., Easley, K. and Green, H. (2000). Targeted ablation of the murine involucrin gene. *J. Cell Biol.* **151**, 381-387.

Elliott, C. E., Becker, B., Oehler, S., Castanon, M. J., Hauptmann, R. and Wiche, G. (1997). Plectin transcript diversity, identification and tissue distribution of variants with distinct first coding exons and rodless isoforms. *Genomics* **42**, 115-125.

Foisner, R., Traub, P. and Wiche, G. (1991). Protein kinase A – and protein kinase C-regulated interaction of plectin with lamin B and vimentin. *Proc. Natl. Acad. Sci. USA* **88**, 3812-3816.

Fontao, L., Favre, B., Riou, S., Geerts, D., Jaunin, F., Saurat, J.-H., Green, K. J., Sonnenberg, A. and Borradori, L. (2003). Interaction of the bullous pemphigoid antigen 1 (BP230) and desmoplakin with intermediate filaments is mediated by distinct sequences within their COOH terminus. *Mol. Biol. Cell* **14**, 1978-1992.

Fuchs, E. and Cleveland, D. (1998). A structural scaffolding of intermediate filaments in health and disease. *Science* **279**, 514-519.
Fuchs, E. and Karakesisoglou, I. (2001). Bridging cytoskeletal interactions. *Genes Dev.* **15**, 1-14.
Fujiwara, S., Kohno, K., Iwamatsu, A., Naito, I. and Shinkai, H. (1996). Identification of a 450-kDa human epidermal autoantigen as a new member of the plectin family. *J. Invest. Dermatol.* **106**, 1125-1130.
Fujiwara, S., Tekeo, N., Otani, Y., Parry, D. A. D., Kunimatsu, M., Lu, R., Sasaki, M., Matsuo, N., Khaleduzzaman, M. and Yoshioka, H. (2001). Epiplakin, a novel member of the plakin family originally identified as a 450-kDa human epiplakin autoantigen. *J. Biol. Chem.* **276**, 13340-13347.
Gallicano, G. I., Bauer, C. and Fuchs, E. (2001). Rescuing desmoplakin function in extra-embryonic ectoderm reveals the importance of this protein in embryonic heart, neuroepithelium, skin and vasculature. *Development* **128**, 929-941.
Green, K. J. and Jones, J. C. (1996). Desmosomes and hemidesmosomes: structure and function of molecular components. *FASEB J.* **10**, 871-881.
Green, K. J., Parry, D. A. D., Steinert, P. M., Virata, M. L. A., Wagner, R. M., Angst, B. D. and Nilles, L. A. (1990). Structure of the human desmoplakins. Implications for function in the desmosomal plague. *J. Biol. Chem.* **265**, 2603-2612.
Guo, L., Degenstein, L., Dowling, J., Yu, Q. C., Wollman, R., Perman, B. and Fuchs, E. (1995). Gene targeting of BPAG1, abnormalities in mechanical strength and cell migration in stratified epithelia and severe neurologic degeneration. *Cell* **81**, 233-243.
Jang, S.-I. and Steinert, P. M. (2002). Loricrin expression in cultured human epidermal keratinocytes is controlled by a complex interplay between transcription factors of the Sp1, CREB, AP1 and AP2 families. *J. Biol. Chem.* **277**, 42268-42279.
Jang, S.-I., Steinert, P. M. and Markova, N. G. (1996). AP1 activity is involved in the regulation of the cell type specific expression from the proximal promoter of the human profilaggrin gene. *J. Biol. Chem.* **271**, 24105-24114.
Kalinin, A., Thoma, N., Iakovenko, A., Heinemann, I., Rostkova, E., Constantinescu, A. and Alexandrov, K. (2001). Expression of mammalian geranylgeranyltransferase type-II in Escherichia coli and its application for in vitro prenylation of Rab proteins. *Protein Expr. Purif.* **22**, 84-91.
Karashima, T. and Watt, F. M. (2002). Interaction of periplakin and envoplakin with intermediate filaments. *J. Cell Sci.* **115**, 5027-5037.
Kazerounian, S., Uitto, J. and Aho, S. (2002). Unique role for the periplakin tail in intermediate filament association: specific binding to keratin 8 and vimentin. *Exp. Dermatol*. **11**, 428-438.
Koch, P. J., de Viragh, P. A., Scharer, E., Bundman, D., Longley, M. A., Bichenbach, J., Kawachi, Y., Suga, Y., Zhou, Z., Huber, M. et al. (2000). Lessons from loricrin-deficient mice: compensatory mechanisms maintaining skin barrier function in the absence of a major cornified envelope protein. *J. Cell Biol.* **151**, 389-400.
Kowalczyk, A. P., Bornslaeger, E. A., Norvell, S. M., Palka, H. L. and Green, K. J. (1999). Desmosomes: intercellular adhesive junctions specialized for attachment of intermediate filaments. *Int. Rev. Cytol.* **185**, 237-302.
Lee, S., Harris, K. L., Whitington, P. M. and Kolodziej, P. A. (2000). Short stop is allelic to kakapo, and encodes rod-like cytoskeletal-associated proteins required for axon extension. *J. Neurosci.* **20**, 1096-1108.
Leung, C. L., Liem, R. K., Parry, D. A. and Green, K. J. (2001). The plakin family. *J. Cell Sci.* **114**, 3409-3410.
Leung, C. L., Green, K. J. and Liem, R. K. H. (2002). Plakin, a family of versatile cytolinker proteins. *Trends Cell Biol*. **12**, 37-45.
Ma, A. S. and Sun, T.-T. (1986). Differentiation-dependent changes in the solubility of a 195-kD protein in human epidermal keratinocytes. *J. Cell Biol.* **103**, 41-48.
Määttä, A., DiColandrea, T., Groot, K. and Watt, F. M. (2001). Gene targeting of envoplakin, a cytoskeletal linker protein and precursor of the epidermal cornified envelope. *Mol. Cell. Biol.* **21**, 7047-7053.
Meng, J. J., Bornslaeger, E. A., Green, K. J., Steinert, P. M. and Ip, W. (1997). Two-hybrid analysis reveals fundamental differences in direct interactions between desmoplakin and cell type-specific intermediate filaments. *J. Biol. Chem.* **272**, 21495-21503.
Nemes, Z., Marekov, L. N. and Steinert, P. M. (1999). Involucrin cross-linking by transglutaminase 1. *J. Biol. Chem.* **274**, 11013-11021.
Ruhrberg, C. and Watt, F. M. (1997). The plakin family: versatile organizers of cytoskeletal architecture. *Curr. Opin. Genet. Dev*. **7**, 392-397.
Ruhrberg, C., Hajibagheri, M. A., Simon, M., Dooley, T. P. and Watt, F. M. (1996). Envoplakin, a novel precursor of the cornified envelope that has homology to desmoplakin. *J. Cell Biol.* **134**, 715-729.
Ruhrberg, C., Hajibagheri, M. A., Perry, D. V. and Watt, F. M. (1997). Periplakin, a novel component of the cornified envelopes and desmosomes that belongs to the plakin family and forms complexes with envoplakin. *J. Cell Biol.* **139**, 1835-1849.
Seifert, G. J., Lawson, D. and Wiche, G. (1992). Immunolocalization of the intermediate filament-associated protein plectin at focal contacts and actin stress fibers. *Eur. J. Cell Biol.* **59**, 138-147.
Simon, M. and Green, H. (1984). Participation of membrane-associated proteins in the formation of the cross-linked envelope of the keratinocyte. *Cell*. **36**, 827-834.
Spazierer, D., Fuchs, P., Pröll, V., Janda, L., Oehler, S., Fischer, I., Hauptmann, R. and Wiche, G. (2003). Epiplakin gene analysis in mouse reveals a single exon encoding a 725 kDa protein with expression restricted to epithelial tissues. *J. Biol. Chem.* **278**, 31657-31666.
Stappenbeck, T. S. and Green, K. J. (1992). The desmoplakin carboxyl terminus coaligns with and specifically disrupts intermediate filament networks when expressed in cultured cells. *J. Cell Biol.* **116**, 1197-1209.
Stappenbeck, T. S., Bornslaeger, E. A., Corcoran, C. M., Luu, H. H., Virata, M. L. and Green, K. J. (1993). Functional analysis of desmoplakin domains, specification of the interaction with keratin versus vimentin intermediate filament networks. *J. Cell Biol.* **123**, 691-705.
Stappenbeck, T. S., Lamb, J. A., Corcoran, C. M. and Green, K. J. (1994). Phosphorylation of the desmoplakin COOH terminus negatively regulates its interaction with keratin intermediate filament networks. *J. Biol. Chem.* **269**, 29351-29354.
Steinbock, F. A., Nikolic, B., Coulombe, P. A., Fucks, E., Traub, P. and Wiche, G. (2000). Dose-dependent linkage, assembly inhibition and disassembly of vimentin and cytokeratin 5/14 filaments through plectin's intermediate filament-binding domain. *J. Cell Sci.* **113**, 483-491.
Steinert, P. M., Parry, D. A. D. and Marekov, L. N. (2003). Trichohyalin mechanically strengthens the hair follicle. *J. Biol. Chem.* **278**, 41409-41419.
Takeo, N., Wang, W., Matsuo, N., Sumiyoshi, H., Yoshioka, H. and Fujiwara, S. (2003). Structure and heterogeneity of the human gene for epiplakin (EPPK1). *J. Invest. Dermatol.* **121**, 1224-1225.
Tijsterman, M., Ketting, R. F. and Plasterk, R. H. (2002). The genetics of RNA silencing. *Annu. Rev. Genet.* **36**, 489-519.
van den Heuvel, A. P., de Vries-Smits, A. M., van Weeren, P. C., Dijkers, P. F., de Bruyn, K. M., Riedl, J. A. and Burgering, B. M. (2002). Binding of protein kinase B to the plakin family member periplakin. *J. Cell Sci*. **115**, 3957-3966.
Wiche, G. (1998). Role of plectin in cytoskeleton organization and dynamics. *J. Cell Sci.* **111**, 2477-2486.
Wiche, G., Krepler, R., Antlieb, U., Pytela, R. and Denk, H. (1983). Occurrence and immunolocalization of plectin in tissues. *J. Cell Biol.* **97**, 887-901.
Wiche, G., Gromov, D., Donovan, A., Castañón, M. J. and Fuchs, E. (1993). Expression of plectin mutant cDNA in cultured cells indicates a role of COOH-terminal domain in intermediate filament association. *J. Cell Biol.* **121**, 607-619.
Yamada, S., Wirtz, D. and Coulombe, P. A. (2003). The mechanical properties of simple epithelial keratins 8 and 18, discriminating between interfacial and bulk elasticities. *J. Struct. Biol.* **143**, 45-55.
Yang, Y., Dowling, J., Yu, Q.-C., Kouklis, P., Cleveland, D. W. and Fuchs, E. (1996). An essential cytoskeletal linker protein connecting acting microfilaments to intermediate filaments. *Cell.* **86**, 655-665.
Yang, Y., Bauer, C., Strasser, G., Wollman, R., Julien, J. P. and Fuchs, E. (1999). Integrators of the cytoskeleton that stabilize microtubules. *Cell* **98**, 229-238.

Journal of Cell Science